STATE OF THE ART IN EM FIELD COMPUTATION*

C. Ng, V. Akcelik, A. Candel, S. Chen, N. Folwell, L. Ge, A. Guetz, H. Jiang, A. Kabel,
L.-Q. Lee, Z. Li, E. Prudencio, G. Schussman, R. Uplenchwar, L. Xiao, K. Ko,
SLAC, Menlo Park, CA 94025, USA

Abstract

This paper presents the advances in electromagnetic (EM) field computation that have been enabled by the US DOE SciDAC Accelerator Science and Technology project which supports the development and application of a suite of electromagnetic codes based on the higher-order finite element method. Implemented on distributed memory supercomputers, this state of the art simulation capability has produced results which are of great interest to accelerator designers and with realism previously not possible with standard codes. Examples from work on the International Linear Collider (ILC) project are described.

INTRODUCTION

The Office of Science in the US DOE is promoting the use of High Performance Computing (HPC) in projects relevant to its mission via the Scientific Discovery through Advanced Computing (SciDAC) program which began in 2001[1]. Since 1996, SLAC has been developing a parallel accelerator modeling capability first under the DOE Grand Challenge and now SciDAC, for use on HPC platforms to enable the large-scale electromagnetic simulations that are needed for improving existing facilities and optimizing the design of future machines.

PARALLEL FE EM CODES

Standard software used for electromagnetic modeling of accelerating cavities and components like CST's family of codes (MAFIA, MWS) are based on a structured, finite difference (FD) grid while others, including Ansoft's HFSS for example, are formulated on the unstructured, finite element (FE) grid. The FE grid allows conformal meshing of curved surfaces providing higher order of accuracy. But none of these codes, to our knowledge, can make use of the significantly larger compute power and memory available on distributed memory supercomputers. As a result in cases where high resolution, system level modeling is necessary, they face limitation on computer memory or require prohibitively long simulation time.

Over the past decade, SLAC has been working on the development of parallel electromagnetic software using higher-order tetrahedral elements. Presently the suite of codes includes:

(1) **Omega3P** – complex eigensolver for finding normal modes in damped cavities;
(2) **S3P** – frequency domain code to evaluate S parameters of RF structures;
(3) **T3P** – time-domain solver to compute transients of driven response and wakefields due to beams;
(4) **Track3P** – particle tracking code for calculating dark current and multipacting.

Under development are:
(1) **Gun3P** – static solver with particles to model formation and transport of DC beams;
(2) **Pic3P** – particle-in-cell code to simulate RF guns and klystrons.

The first application of SLAC's parallel FE EM codes dates back to the NLC structure R&D where the required accuracy of 0.01% in the accelerating frequency of the Damped, Detuned Structure (DDS) was met using **Omega3P**. Since then, the codes have been applied to many accelerator projects, ranging from linacs to cyclotrons, and from PEP-II to the LCLS. This paper presents results from simulations devoted to the International Linear Collider to introduce the usefulness and unique features of this advanced approach.

HIGHER ORDER FE AND PARALLELISM

To demonstrate the power of the parallel higher-order FE method, consider the end group of the ILC Low-Loss (LL) cavity design consisting of the end cell, an input coupler at the enlarged end-pipe, and the beampipe (Fig.1 Left). The model was simulated with **Omega3P** using linear (p=1), quadratic (p=2) and cubic (p=3) elements. In Fig. 1 (Right) the % error in the fundamental mode frequency (1.3 GHz) is plotted versus the computer memory required. It can be seen that the required memory is significantly less for higher order elements (e.g. quadratic versus linear) to achieve the same accuracy. For an error of 20 kHz error out of 1.3 GHz, 67,000 quadratic elements were used in the model which took less than 1 minute to run on 16 CPUs requiring 6 GB memory.

Even with quadratic elements, it is evident that modeling accurately an entire 9-cell SRF cavity complete with HOM couplers (Figs. 2 and 3) would require memory far greater than what is available on a single CPU. Hence parallel processing becomes absolutely essential, and also provides the additional benefit of linear speedup (1/N, N being the number of processors) which significantly reduces simulation time.

Figure 1: (Left) FE mesh of the LL cavity end group: end cell, input coupler, beampipe, (Right) comparison of error convergence (in %) versus computer memory for three orders of FE elements (linear, quadratic and cubic).

HOM DAMPING IN THE ILC LL CAVITY

The Low-Loss cavity design [2] (Figs. 2 and 3) is being considered as a possible upgrade to the baseline TESLA cavity for the main linac of the ILC. Based on a different cell shape, it has 20% lower cryogenic loss plus higher gradient (via a smaller beampipe) over the TESLA design. Additionally, the endpipes where the couplers are located are larger which now allow modes higher than the 2nd dipole band to propagate and be damped. Using the HOM coupler from the TESLA cavity directly, **Omega3P** analysis found that the 1st mode in the 3rd dipole band does not meet the beam stability requirement of $Q_e < 10^5$.

Figure 2: **Omega3P** mesh of the ILC LL cavity design.

Figure 3: (Left) HOM coupler at the input end, (Middle) details of the HOM coupler geometry, (Right) input and HOM couplers at the output end.

A high fidelity mesh consisting of 0.53M quadratic elements (3.5M DOFs) was used to model the cavity. This provides sufficient resolution for modifying the end groups to improve the HOM damping. By adjusting the end-pipe radius, the HOM coupler azimuthal location, and the loop shape and configuration, the Q_e of the dangerous 3rd band mode was reduced to below the stability threshold. The **Omega3P** simulations were performed on the IBM SP (Seaborg) at NERSC using a direct solver, requiring 300 GB memory on 512 processors and 1 hour of runtime per dipole band. Comparison between original and new damping results is shown in Fig. 4. Similar improvement has been made to KEK's ICHIRO cavity which is based on the LL design.

Figure 4: (Top) Qe versus frequency for the LL cavity with TESLA HOM coupler (blue) and SLAC's improved design (red), (Bottom) R/Q for the same dipole bands.

SIMULATIONS OF THE TDR CAVITY

In Time Domain

The temporal EM field behavior in the ILC baseline TDR (TESLA) cavity due to a beam transit was simulated with **T3P** to obtain useful information on the transients in the cavity and the 3D effects from the couplers (input and HOM) on the short range wakefields. Fig. 5 shows two snapshots in time of the magnetic fields (image current) on the cavity wall induced by the transiting beam: the first set of pictures from before the beam enters the cavity and the second set after the beam has passed. Performed on Seaborg, the **T3P** simulation parameters are as follows: 1.75M quadratic elements (10M DOFs) requiring 173 GB on 1024 processors and 47 minute per ns of beam travel.

Figure 5: Snapshots of **T3P** magnetic field contours on the wall surface of the TDR cavity and couplers before beam enters main cavity (Top set) and after exiting output end beampipe (Bottom set).

Figure 6: Dipole mode spectrum showing damping of the 1st dipole band (Left) and 2nd dipole band (Right), with **Omega3P** results in black, and measurements from 8 TESLA cavities in color.

In Frequency Domain

The TDR cavity was actually the first application of the SLAC tools to the ILC because plenty of measured data

05 Beam Dynamics and Electromagnetic Fields
D05 Code Developments and Simulation Techniques

on the cavity is available for benchmarking purposes. As with any geometry modeling meshing is crucial to solution accuracy so considerable effort had been devoted to mesh convergence studies. Using a converged mesh with quadratic elements, the dipole mode spectrum calculated by **Omega3P** is compared with measurements from the 8 cavities in an actual TTF cryomodule (Fig. 6).

Cavity Imperfections

In the TDR cavity each dipole band consists of 9 pairs of modes as the mode degeneracy is split by the 3D effect of the couplers. In Fig. 6, the **Omega3P** results are shown in black while the colored cluster around each **Omega3P** pair represents the measured data from the 8 cavities in an actual TTF cryomodule. Let us focus on the 6th mode in the second band which is plotted in Fig. 7. Compared with the ideal cavity simulated by **Omega3P** the measurements reveal that in real cavities: (1) the splitting of the mode pair is larger, (2) the mode pair is mostly shifted to lower frequencies, and (3) their Qe's are scattered toward the high side. This Qe increase would be problematic if their values exceed the beam stability limit. We attribute the differences between the simulation and measurement to cavity imperfections. Recognizing that deformations are playing a major role, we have embarked on an effort to determine the true cavity shape by solving an inverse problem [3]. We use the data from the TESLA data bank [4] such as frequencies and field amplitudes as input parameters. The goal is to identify the critical dimensions affecting Qe and study their sensitivity to deformations.
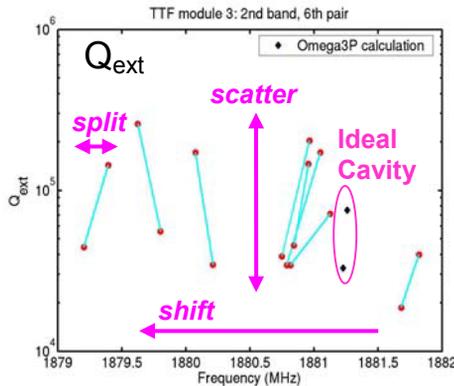
Figure 7: Comparison between ideal cavity results from **Omega3P** and measurements from 8 different TESLA cavities in an actual cryomodule, showing differences in mode splitting, mode frequencies and damping.

Mode Rotation

In analyzing the fields of the dipole modes in the TDR cavity as computed by **Omega3P**, a new mode rotation effect was discovered. This occurs when the modes of a degenerate mode pair split by 3D effects (input and HOM couplers or imperfections) couple to each other through the overlap of their finite line widths due to damping [5]. As a result, the two modes become elliptically polarized and they rotate in time (see Fig. 8). Impact of this effect on the beam dynamics is being investigated.
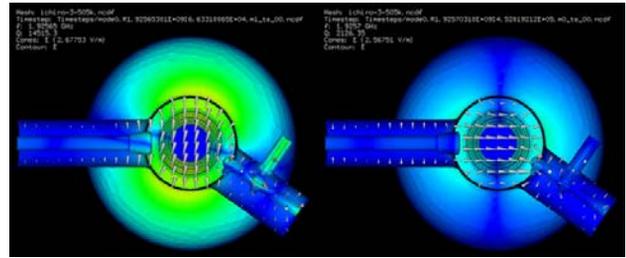
Figure 8: Snapshot in time of two rotating modes forming the 6th pair in the 2nd dipole band coupled through the overlap of their finite line widths due to damping.

SUPPORT OF ICHIRO CAVITY R&D

Multipacting Effect

Researchers at KEK are devoting a large effort to high gradient cavity R&D for the ILC with the focus on the ICHIRO cavity [6] which evolved from the LL cavity design. In single cell tests, the ICHIRO design established a record gradient of 54 MV/m. However, 9-cell ICHIRO cavities (Fig. 9) are having difficulties reaching gradients greater than 30 MV/m. The ICHIRO cavity differs from the LL design in the enlarged end-tube at the input end. SLAC simulated multipacting in the ICHIRO cavity with **Track3P** and found MP activity in the transition from the enlarged end-tube to the beamipe. The calculated MP levels are found to be in agreement with X-ray barriers observed in experiments (see Fig. 10). Work is underway to redesign the cavity to circumvent this problem.

Figure 9: Prototype of ICHIRO cavity under high power processing at KEK with enlarged end-tube shown on the input end to the left.

SLAC simulated MP levels [MV/m]	ICHIRO#0 X-ray barrier [MV/m]
	7.4, 9.0, 7-17
12.0	11-29.3, 12-18
13.9	13, 14, 14-18, 13-27, 13-27
16.8	(17, 18)
21.2	20.8
29.4	28.7, 29.0, 29.3, 29.4
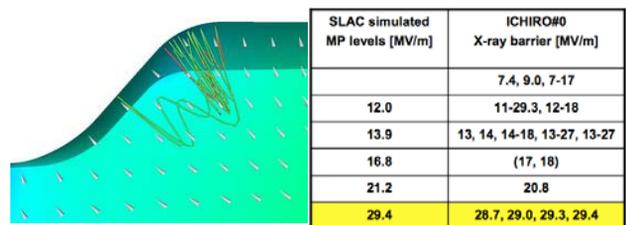
Figure 10: (Left) Snapshot in time of multipacting at the transition from enlarged end-tube to beampipe in the ICHIRO prototype, (Right) comparison between **Track3P** results and KEK measurements.

HOM Notch Filter

The notch filter in the HOM coupler is designed to reject the fundamental mode power. It is of great interest to find out its sensitivity with respect to the notch gap dimensions and the detuning effect off the fundamental frequency at 1.3 GHz. As noted previously, the HOM

coupler has a complex geometry with feature size (notch gap of order 1 mm, pickup gap < 1 mm) much smaller than the cavity size (diameter 200 mm). It would have been impossible to model the fields in the HOM coupler correctly without the combined high accuracy of conformal meshing, increased local resolution, and quadratic elements (see Fig. 11 Left).

To understand the sensitivity and detuning effect of the HOM notch filter two calculations were carried out. First the tuning curves of the HOM coupler for three different notch gap dimensions were computed with **S3P** to find the response around the fundamental mode frequency of 1.3 GHz (Fig. 11 Right) and a sensitivity of 0.11 MHz per micron was obtained. Next, the fundamental mode was calculated for the cavity equipped with HOM couplers set at the three different notch gap dimensions. A comparison of the fields in the HOM couplers from the three fundamental modes is shown in Table 1. We see that the notch gap fields vary little in the three cases. However, the Qe of the mode is reduced by orders of magnitude when the notch filter is tuned far off the mode frequency. This leads to large amount of power flowing through the pickup feedthrough and could result in excessive heating if proper cooling is not engineered into the design.
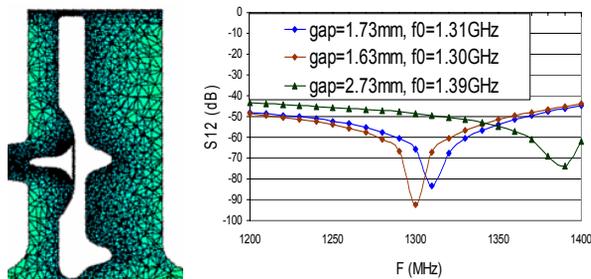
Figure 11: Detailed mesh in the ICHIRO HOM coupler showing mesh density in the notch gap and near the antenna tip, (right) tuning curves of HOM coupler with three different notch gaps near 1.3 GHz.

Table 1: Field values in the notch gap and at the antenna tip for three different notch gap dimensions. Current through the pickup line is sensitive to notch gap tuning.

Notch gap (mm)	Notch gap field (MV/m)		Antenna tip Field (MV/m)		Qext of HOM port @1.3GHz	
	Up-stream	Down-stream	Up-stream	Down-stream	Up-stream	Down-stream
1.63	16.9	5.0	0.8	0.2	6.1e+9	1e+12
1.73	16.5	4.9	1.4	0.4	5.2e+8	9.e+9
2.73	13.3	3.9	6.1	3.0	1.4e+7	1.7e+8

MULTI-CAVITY STRUCTURES

The advantage of parallel processing becomes obvious when multi-cavity structures are considered. First studied at DESY, the superstructure design combines two or more cavities through weakly coupled beampipes into a single unit. The goal is to reduce the number of input couplers and increase the packing factor which reduces the linac length. One concern with superstructures is the presence

of trapped modes between cavities. Fig. 12 shows a two-cavity superstructure model and an HOM mode trapped between the cavities as computed by **Omega3P.** In the effort towards simulating DESY's TTF cryomodule consisting of eight TESLA cavities (Fig. 13), a four-cavity structure was modeled to find the HOM mode spectrum and one such mode is shown in Fig. 15. Beamline absorbers will be included in the model for the cryomodule to evaluate their effectiveness in damping the modes above the beampipe cutoff. This simulation will be carried out in the time domain using **T3P.**
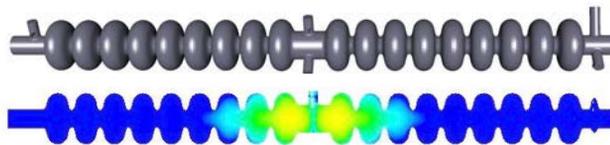
Figure 12: Two-cavity superstructure model and a trapped mode as computed by **Omega3P.**
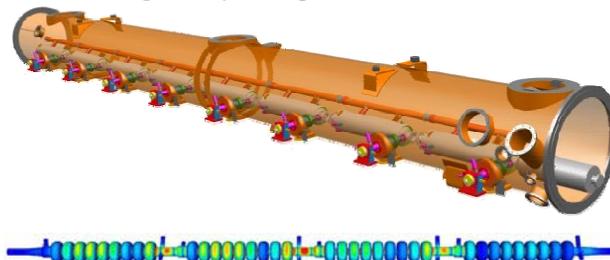
Figure 13: DESY 8-cavity TTF cryomodule model and an HOM mode in a four-cavity structure from **Omega3P.**

The simulation parameters for the four-cavity structure on Seaborg are: 2.5M quadratic elements (15M DOFs) requiring 276 GB on 768 CPUs and 10 hours of runtime for 2 modes. In order to simulate the large structure, an iterative linear solver was used to reduce the memory requirement.

PARALLEL FE PARTICLE CODES

An important area of particle accelerator technology involves RF devices such as klystrons and RF guns. We are developing advanced tools for designing and analyzing these devices. Consistent with the rest of the SLAC software suite, these codes, **Gun3P** and **Pic3P**, are based on FE unstructured grids and are designed to run on distributed memory computers. Again, the rationale is higher accuracy in fields, increased beam resolution, larger problem size (end-to-end simulation) and faster turnaround time.

The target application for **Gun3P** is the gun for the sheet beam klystron, presently under development at SLAC as a possible RF source to drive the ILC main linac. Codes currently in use for modeling the gun are not parallel so simulation time can become longer than desirable. A parallel capability would overcome this bottleneck and open up the possibility for an end-to-end simulation that can include both the beam formation at the gun and the beam transport through the klystron circuit.

05 Beam Dynamics and Electromagnetic Fields
D05 Code Developments and Simulation Techniques

Fig. 14 shows the preliminary results from **Gun3P** on the static electric fields in the sheet beam gun cavity. Inclusion of beam trajectories is in progress.
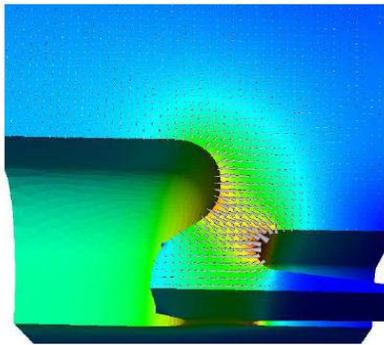
Figure 14: Static electric field in the ILC sheet beam gun cavity as computed by **Gun3P**.

The Particle-In-Cell (PIC) method is a commonly used approach for self-consistent simulation of electromagnetic field and charged particle interaction. Most PIC codes are formulated on the orthogonal FD grid because the implementation is straight forward, although some have succeeded with non-orthogonal grids to provide better geometry accuracy. We have made good progress in implementing the PIC method on a 2D unstructured grid valid for second order elements (**Pic2P**). In benchmark runs on the LCLS RF gun design [7] (Fig. 15), **Pic2P** exhibits higher accuracy with fewer particles and less field unknowns when compared with MAFIA results (Fig. 16). Using quadratic elements for better geometry representation and field accuracy, a **Pic2P** run takes 2 hours on a Xeon 3.4 GHz machine for a mesh with 150K DOFs and 100K to reach convergence. In comparison, a MAFIA run time is similar for a mesh with 6M DOFs and 200K particles for getting close to convergence. The extension to 3D (**Pic3P**) for which parallel processing will be essential is underway. When completed, **Gun3P** and **Pic3P** will provide a set of new design tools for the ILC sheet beam klystron.
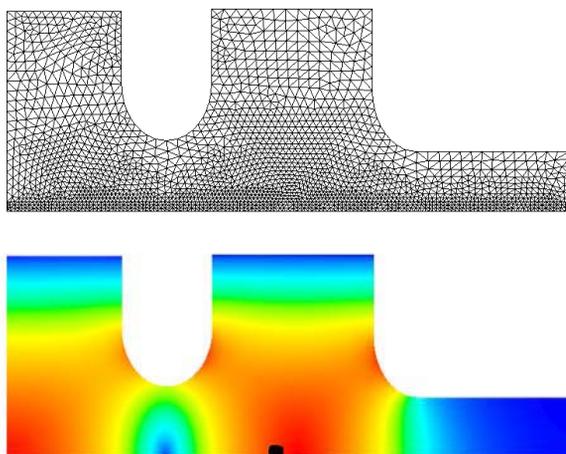
Figure 15: (Top) Triangular elements in the LCLS gun mesh, (Bottom) snapshot in time of charged bunch shown with fields in the LCLS gun cavity.
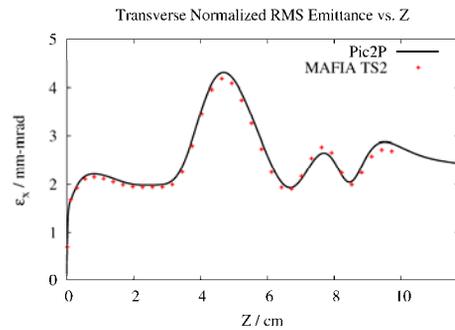
Figure 16: Comparison of the emittance of the LCLS RF gun using **Pic2P** and MAFIA (see text for details).

CONCLUSION

Higher order finite elements and parallel processing have enabled EM field computation to reach a level of realism and accuracy not previously attainable, and have allowed accelerator applications to progress from single component modeling to simulation at the system scale. The impact of SLAC's suite of parallel FE codes on the ongoing ILC R&D is described. Not covered in this paper are the advances in computational science which are the key ingredients in making this work possible. These SciDAC supported efforts include research in meshing, nonlinear eigensolver, optimization, adaptive refinement, and visualization.

ACKNOWLEDGEMENTS

REFERENCES

[1] K. Ko et.al., SciDAC and the International Linear Collider: Petascale Computing for Terascale Acelerator, Proc. SciDAC 2006 Conference, Denver, Colorado, June 25-29, 2006

[2] J. Sekutowicz et.al., Design of a Low Loss SRF Cavity for the ILC, Proc. PAC 2005, Knoxville, Tennessee, May 12-16, 2005.

[3] V.Akcelik et.al., Adjoint Methods for Electroma-gnetic Shape Optimization of the Low-Loss Cavity for the International Linear Collider, Proc. SciDAC 2005 Conference, San Francisco, California, 2005.

[4] G. Kreps, private communications.

[5] K. Ko et.al., Advances in Electromagnetic Modeling through High Performance Computing, Proc. SRF Workshop 2005, Cornell University, July 10-15, 2005.

[6] T. Saeki et.al., Fabrication of Four 9-cell Ichiro High-Gradient Cavities for the R&D of ILC Accelerator in KEK, Proc. SRF Workshop 2005, Cornell University, July 10-15, 2005.

[7] L. Xiao et.al., Dual Feed RF Gun Design for the LCLS, Proc. PAC 2005, Knoxville, Tennessee, May 15-20, 2005.